

BEHAVIOR OF FOOTING GROUP RESTING ON COLLAPSIBLE SOIL BASED ON EXPERIMENTAL AND NUMERICAL STUDY

Tarek M. Abdelaziz⁽¹⁾, Ashraf k. Nazir⁽²⁾, Ahmed M. Ragheb⁽³⁾ and GehAD E. Saad⁽⁴⁾

(1) Professor, Department of Construction and Building Engineering, Arab Academy for Science, Technology and Maritime Transport, Alexandria, Egypt, tareqmaziz@aast.edu

(2) Professor, Department of Civil Engineering, Tanta University, Egypt, ashraf.Nazir@f-eng.tanta.edu.eg

(3) Associate Professor, Department of Construction and Building Engineering, Arab Academy for Science, Technology and Maritime Transport, Alexandria, Egypt, aragheb@aast.edu

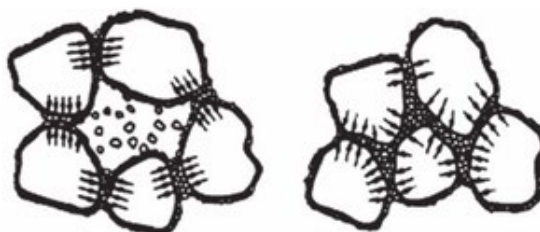
(4) Graduate Student, Department of Construction and Building Engineering, Arab Academy for Science, Technology and Maritime Transport, Alexandria, Egypt, gehadelsayed336@gmail.com

Keywords: Collapsible soil, collapse settlement, PLAXIS, group of footings, wetted depth, distribution of water content.

1. **ABSTRACT:** This study deals with identifying the behavior of contiguous square footing groups subjected to rainfall water. A variety of parameters were represented in order to study the effect of these parameters on the behavior of the footing group. The tests were conducted in a wide tank with collapsible soil and models of square footing groups. Using the experimental model to investigate the collapse settlement due to the infiltration of rainfall water through collapsible soil beneath contiguous square footing. In addition, the distribution of water content and the depth of wetting were measured. Moreover, numerical models were carried out by PLAXIS 3D V21 to simulate experimental models. From the test results, it was noticed that increasing the number of footings in a group causes a decrease in settlement.

2. INTRODUCTION

Collapsible soil is considered to be one of the problematic soils, alongside other problematic foundation materials such as expansive soil or peat. Collapsible soil has incredible strength when dry, but once wet, it loses strength and volume, regardless of loading. The sudden and severe volume change might cause extensive structural damage. As a result, a proper understanding of the behavior of this soil is required for safe and cost-effective geotechnical designs (Choudhury and Bharat, 2015). Collapsible soils, such as loess sands, are predominantly composed of silt-sized particles loosely organized in a cemented honeycomb structure Figure (1). Small quantities of water-softening or water-soluble cementing agents, including clay minerals and calcium carbonate, hold the loose structure together. Water dissolves or weakens the bonds between silt particles, allowing them to pack more densely under any compressive pressure (Lawton et al., 1992). Soil particles, permeability, saturation, initial void ratio, over-consolidation ratio (OCR), and collapsible layer thickness all influence the amount of settlement or collapse (Kalantari, 2013).

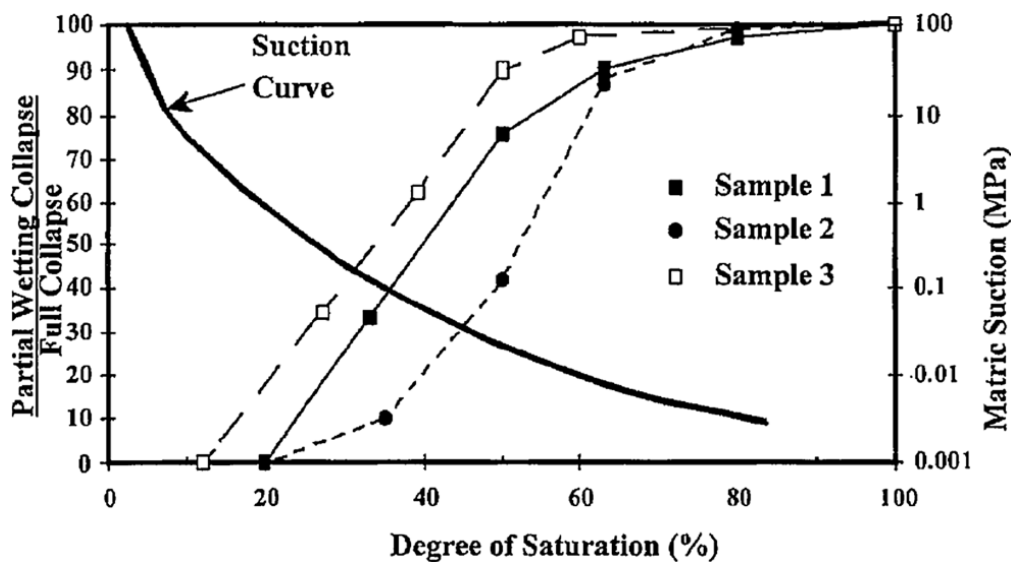


(a) Dry soil with honeycombed structure
before inundation

(b) Soil structure after inundation

Figure(1): Loaded hydro-collapsible soil before (a) and after (b) inundation with water
(after Lawton et al., 1992).

Houston et al. (2001) identified collapsible soils as moisture-sensitive. According to their research, increasing moisture content in collapsible soils leads to higher deformations and settlements. Additionally, because these soils have easy access to water, they suffer to collapse. Houston et al. (2001) measured collapse settlement in three types of collapsible soils (1, 2, and 3) to determine settlement amounts for partial to full wetting. Figure (2) shows that vertical deformations for all three samples are strongly related to their saturation degree, with more moisture content resulting in greater settlement. Figure 2 demonstrates that when all three collapsible soil samples achieve complete saturation (100%), the maximum collapse strain (partial wetting collapse/full collapse) or failure circumstances occur. According to Murthy (2010), the amount of collapse in collapsible soils depends on the relative proportions of each component, such as saturation degree, initial void ratio, material stress history, collapsible stratum thickness, and applied load.



Figure(2): Partial collapse owing to partial wetting- for three types of soils (after Houston et al. ,2001).

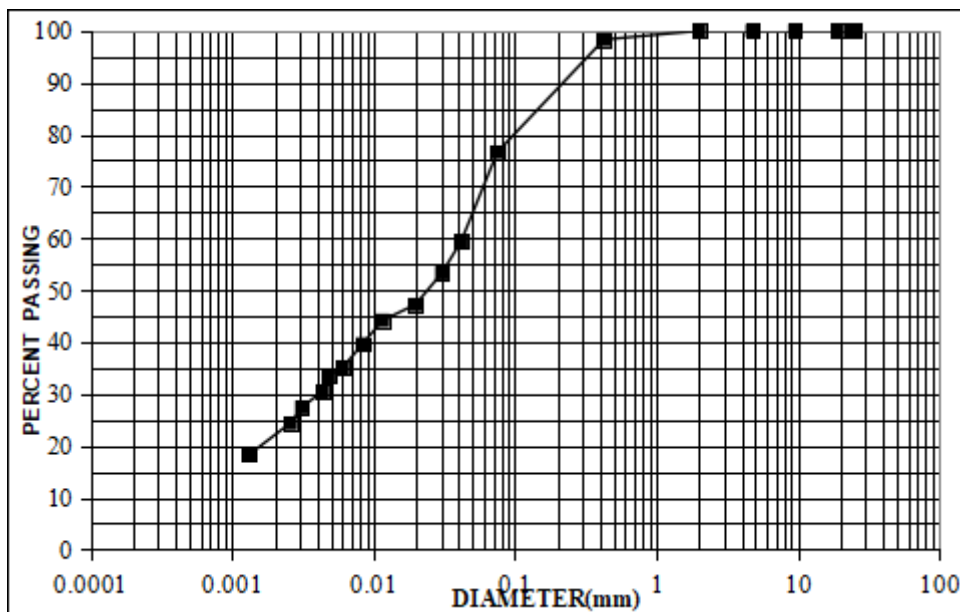
Walsh et al. (1993) created suction contours for a location to determine the degree of soil moisture. The underlying soils at the location have a wide range of fines content. A method for calculating suction values using geotechnical testing results was published. They stated that the most significant factors in wetting sensitive soil are the source of water and the extent of wetness. Sources can be quantified using records. However, the extent of wetting is measurable rather than projected. Moreover, Addabbo and Abdelaziz (2006) conducted laboratory infiltration tests using rainfall simulation to predict the extent of the wetting zone surrounding and under a footing model resting on collapsible soil. The studies allowed for real-time monitoring of moisture distribution beneath and around the footing, and it was indicated that while the wetted zone was not horizontal during the early infiltration phases, it did develop a horizontal profile beyond a certain time limit. The limiting time for the early wetting stage was discovered to be dependent on soil factors in addition to footing size. Furthermore, Ali (2021) carried out a field case study to expect collapse duration and stress-settlement relationship while taking into account depth, thickness of collapsible layer, natural structure, added loads, water flow, and irrigation. In the proposed actual case study, the fluctuation in collapsing soil water content is confined to a depth no greater than four times the foundation width. The results showed that, under certain initial saturation conditions, further wetness may produce more settlement due to particle rearrangement and reduce soil suction. Also, Fattah and Dawood (2020) conducted a laboratory investigation on three types of gypseous soils from various locations of Iraq to estimate volume changes and collapse potential (CP) related with variations in soil suction using a pressure cell and the influence of initial load on soil suction. A variety of collapse experiments were conducted utilizing the oedometer device [single oedometer test (SOT) and double oedometer test (DOT)]. In addition, a large-scale model with soil dimensions of 700 _ 700 _ 600 mm was utilized to demonstrate the impact of water content variations in various relationships (collapse with time, stress with time, suction with time). The collapse potential determined from laboratory testing (collapse tests) is greater than that measured from large models, as reported by Houston et al. (2002). The volume change dropped dramatically after inundation because to the reduction in matric suction. After 24 hours of inundation, the volume change becomes constant when the suction is reduced to zero. Ali (2021) conducted a single odometer test in the lab and a plate load test with pseudo-consolidation test in the field, utilizing four locations in BORG AL-ARAB. The research focuses on the parameters that influence the assessment of collapse potentials, including particle size distribution, void ratio, degree of saturation, and natural density. The results found that, for the same undisturbed block samples for all examined locations, the collapse potential calculated in the field are smaller than those anticipated in the laboratory by (15-16%). When working with collapsible soils, geotechnical engineers encounter numerous significant obstacles. These include (a) Identify and characterize collapsible soil places, (b) Estimate the extent and degree of wetness, (c) Estimate collapse stresses and settlements, and (d) Choosing design and mitigation alternatives (Houston et al., 2001). Therefore, in this paper, a set of laboratory tests were conducted to study the behavior of collapsible soil beneath a group of square footings subjected to rainfall water on the distribution of water content and depth of wetting, which affect collapse settlement. Moreover, a simulation model was developed to check the ability of PLAXIS 3D V21 to predict the collapse settlement, and results were compared with experimental results.

3. SOIL PROPERTIES

The collapsible soil utilized in this study was taken at a place along the Borg El-Arab Desert Road in the King Marriott area, west of Alexandria, Egypt. The soil was sieved on-site with conventional sieves. The soil sample was air-dried in the lab, and a number of tests were carried out to assess the soil parameters, as shown in table (1). Figure (3) depicted the sample's grain size distribution.

Table (1): The soil properties obtained from experimental tests

Collapsible soil sample characteristics.	
Clay % (<0.005 mm)	33.51
Silt % (0.005 – 0.074 mm)	43.11
Fine sand % (0.074 – 0.425 mm)	21.69
Medium sand % (0.425 – 2.0 mm)	1.69
Coarse sand % (2.0 – 4.75 mm)	0.0
Specific gravity	2.680
Plastic Limit %	N/A (soil is non-plastic)
Liquid Limit %	N/A



Figure(3): The Grain Size Distribution Curve (% of fines = 76.62%).

4. EXPERIMENTAL WORK

In this research, a series of experimental experiments were performed to simulate the contiguous square footing groups subjected to water infiltration through collapsible soil square, as illustrated in figure (4), while taking into account the influence of various factors on the behavior of collapsible soil. The parameters to be evaluated are the including number of footings (N) and intensity of induced water (Qw). The study examined the intensity of induced water (Qw=2 and 3 cm³/cm²), and number of footings (N= 1, 2 and 4). The collapse settlement generated by the infiltration of rainfall water through the soil beneath a loaded square footings model was determined, in addition to the changes in wetting zone geometry and water content distributions caused by parameter variations.

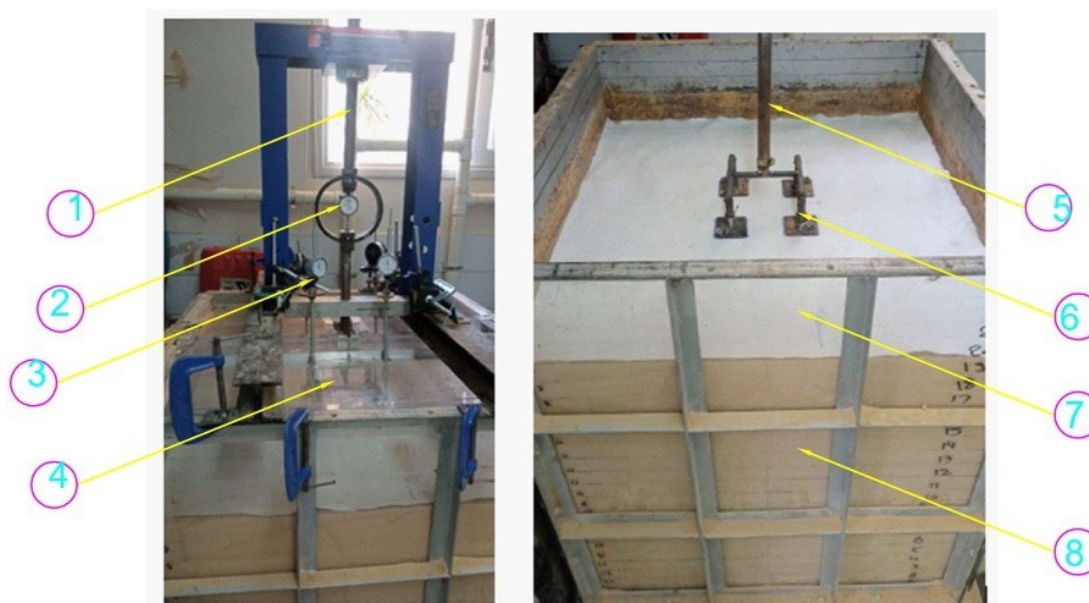


Figure (4): The test setup for infiltration tests.

- 1) Upper loading shaft
- 2) Proving ring
- 3) Dial gauge device
- 4) Water distribution perspex grid
- 5) Lower loading shaft
- 6) Steel plates
- 7) Transparent perspex wall
- 8) Formed soil sample

4.1 Water Infiltration Through Collapsible Soil

Subgrade soils rarely reach complete saturation, except when groundwater levels rise. El-Ehwany and Houstom (1990) noted that high-quality collapse settlement prediction is strongly dependent on an accurate estimation of the depth of the wetness zone. As a result, the depth of the wetness zone front was also assessed, as illustrated in figure (5) and figures (7 and 8). The change in soil water content under the footing model for various parameters was measured in the lab, as demonstrated in figure (6) and figures (9 and 10).



Figure (5): The depth of wetting (D_w) beneath the footing center [$\gamma_d = 14.41 \text{ kN/m}^3$, $F=76.62\%$, $B=7.6 \text{ cm}$, $W_o=3.6\%$, $q=100 \text{ KN/m}^2$, $N= 4$, $Q_w=3 \text{ cm}^3/\text{cm}^2$].



Figure (6): The distribution of water content beneath the center of a group of footing [$\gamma_d = 14.41$ kN/m³, $F=76.62\%$, $B=7.6$ cm, $W_o=3.6\%$, $q=100$ KN/m², $N=4$, $Q_w=2$ cm³/cm²].

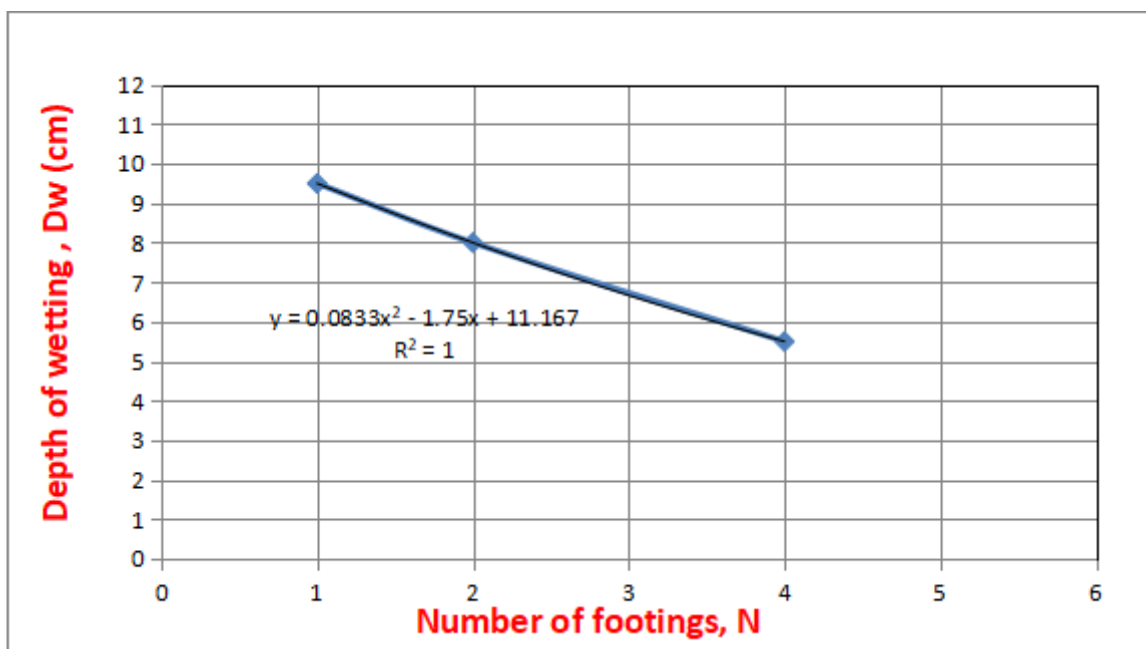


Figure (7): The depth of wetting beneath the center of a group of footings for different number of footings (N) at [$Q_w=2$ cm³/cm², $\gamma_d = 14.41$ kN/m³, $F=76.62\%$, $B=7.6$ cm, $W_o=3.6\%$ and $q=100$ KN/m²].

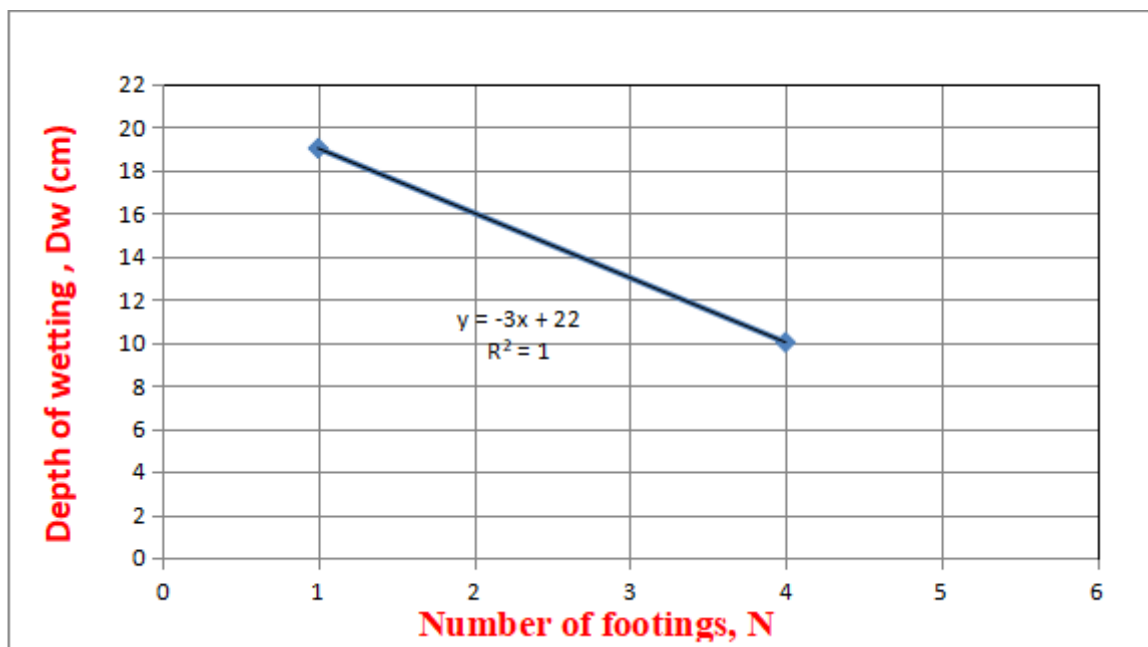


Figure (8): The depth of wetting beneath the center of a group of footings for different number of footings (N) at $[Q_w=3 \text{ cm}^3/\text{cm}^2, \gamma_d = 14.41 \text{ kN/m}^3, F=76.62\%, B=7.6 \text{ cm}, W_o=3.6\%$ and $q=100 \text{ KN/m}^2]$.

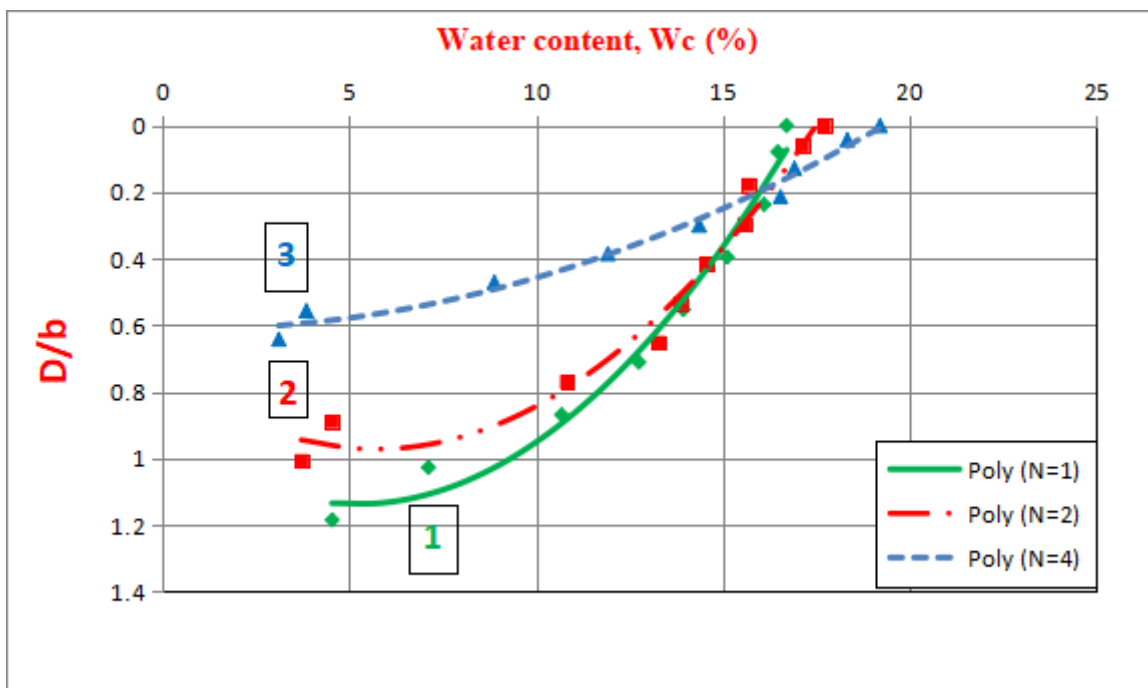


Figure (9): The distribution of water content beneath the center of a group of footings for different number of footings (N) at $[Q_w=2 \text{ cm}^3/\text{cm}^2, \gamma_d = 14.41 \text{ kN/m}^3, F=76.62\%, B=7.6 \text{ cm}, W_o=3.6\%$ and $q=100 \text{ KN/m}^2]$.

1	N=1	$y = -0.008 X^2 + 0.083 X + 0.9221$	$R^2=0.983$
2	N=2	$y = -0.007 X^2 + 0.0797 X + 0.744$	$R^2=0.9745$

3	N=4	$y = -0.0017 X^2 + 0.002 X + 0.6115$	$R^2=0.9835$
---	-----	--------------------------------------	--------------

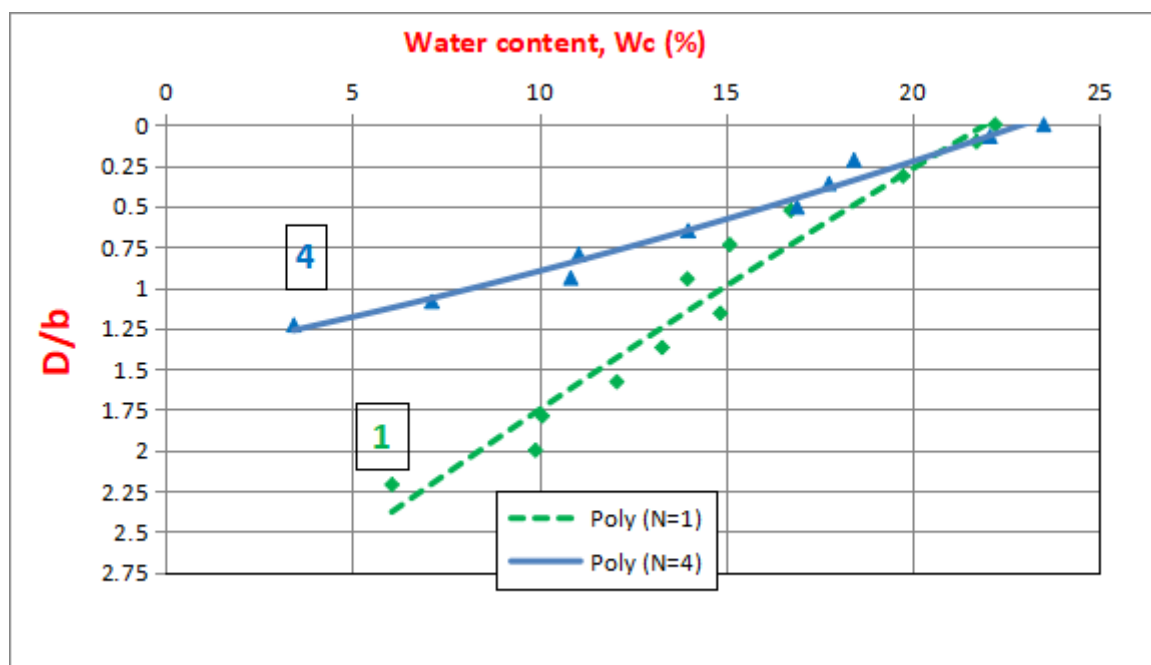


Figure (10): The distribution of water content beneath the center of a group of footings for different number of footings (N) at $[Q_w=3 \text{ cm}^3/\text{cm}^2, \gamma_d = 14.41 \text{ kN/m}^3, F=76.62\%, B=7.6 \text{ cm}, W_o=3.6\% \text{ and } q=100 \text{ KN/m}^2]$.

N=1	$y = -0.0008 X^2 - 0.1716 X + 3.902$	$R^2=0.9525$
N=4	$y = -0.0007 X^2 - 0.0455X + 1.4272$	$R^2=0.9799$

4.2.1 Empirical Equation For The Distribution of Water Content And The Depth of Wetting

5. Based on the laboratory testing findings, the distribution of soil water content under the footing model was assessed at the depth of wetness for various parameters. It can be achieved to develop an empirical equation (1) by using the Curve Expert Professional Program in figure (11) in order to predict the value for distribution of water content with various wetted depths. The results showed that the average ratio of expected to actual water content increase is (1.01). In addition, empirical equation (2) predicts the value for depth of wetting, as shown in figure (12). The average ratio of obtained value to real value is (0.956). Furthermore, the value of wetted density for different wetted depths can be expected by empirical equation (3), as presented in figure (13). The average ratio of estimated value to real value is (1.00).

$$W_c = [a + b * X_1 + c * X_2 + d * X_1^2 + e * X_2^2 + f * X_1^3 + g * X_2^3 + h * X_1 * X_2 + i * X_1^2 * X_2 + j * X_1 * X_2^2]$$

(1)

Where:

$$X_1 = \frac{Q_w * W_o}{q * Fines * \gamma_d * N * B / B_o}$$

$$X2 = Dw/B$$

a	b	c	d	e	f	g	h	i	j
8.66	830	-18	17200	1.74	100 000	- 0.582	1 12	-110	2.88

When calculating the distribution of water content, considering the value of water content equals the value of natural water content at the final wetted depth, and do not use the suggested equation to calculate the water content at this depth.

Figure (11): The Resulting 3D Graph of Wc vs $\frac{Q_w * W_o}{\gamma_d * f_{ines} * q * N * B / B_o}$ and Dw/B

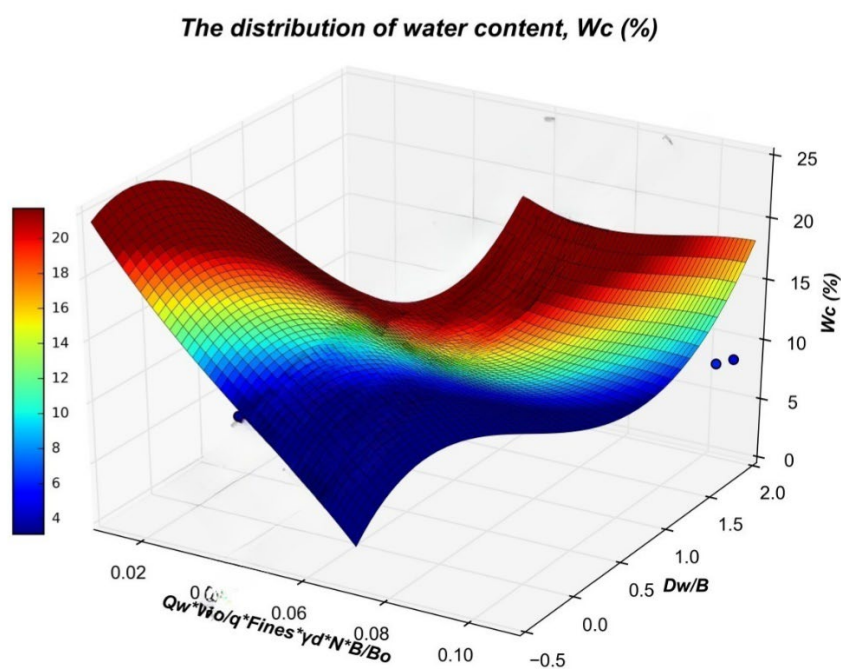


Figure (11): The Resulting 3D Graph of Wc vs $\frac{Q_w * W_o}{\gamma_d * f_{ines} * q * N * B / B_o}$ and Dw/B

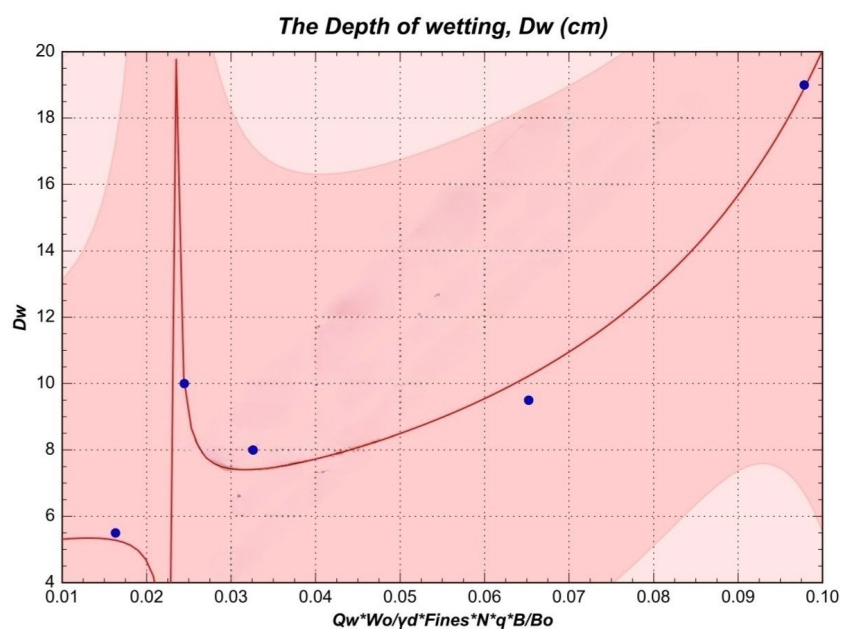


Figure (12): The Depth of wetting (D_w) against X for all parameters.

$$D_w = \frac{a+b*X}{1+c*X+d*X^2} \quad (2)$$

Where:

$$X = \frac{Q_w * W_o}{\gamma_d * Fines * N * q * B/B_o}$$

a	b	c	d
5	-225	-51	320

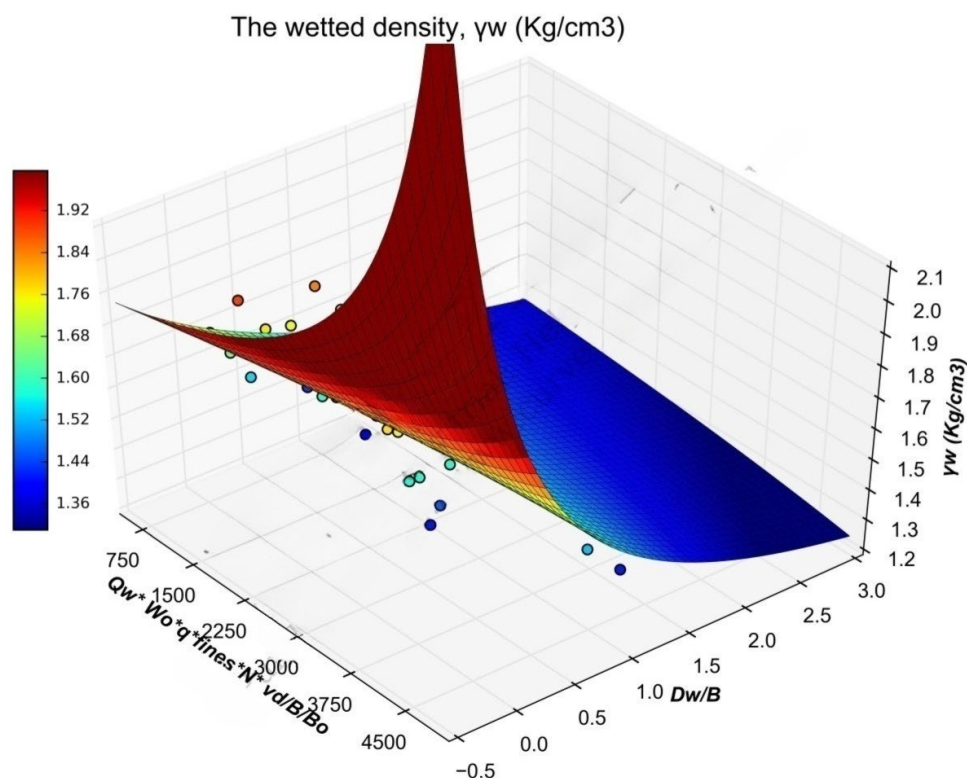


Figure (13): The Resulting 3D Graph of γ_w vs $\frac{Q_w * W_o * q * \text{fines} * N * \gamma_d}{B/B_o}$ and Dw/B

$$\gamma_w = \left[\frac{a + bX_1 + cX_2}{1 + dX_1 + eX_2} \right] \quad (3)$$

Where:

a	b	c	d	e
1.7 2	- 0.000235	0.2 84	- 0.000148	0.2 9

$$X_1 = \frac{Q_w * W_o * q * \text{fines} * N * \gamma_d}{B/B_o}, \quad X_2 = Dw/B$$

γ_w = the wetted density (Kg/cm³).

W_c = the distribution of water content (%)

Dw = the wetted depth (cm)

Q_w = the intensity of induced water (cm³/cm²)

Fines= the percentage of fines that passing sieve No. 200 (%)

W_o = the initial water content (%)

q = the applied stress (Kg/cm^2).

γ_d = the initial dry unit weight of the soil (Kg/cm^3)

B = the footing width (cm)

B_0 = the initial footing width (cm)

N = number of footings.

4.2 Collapse Settlement

A series of experimental tests were conducted to investigate the influence of various factors on the behavior of collapsible soil, and the collapse settlement was calculated as a result of rainfall water beneath the loaded square footings model, as shown in figures (14 and 15). Figures (14) and (15) show the influence of the number of footings at the intensity of induced water ($Q_w = 2$ and $3 \text{ cm}^3/\text{cm}^2$, respectively). The results illustrated that as the number of footings (N) increased, collapse settlement (S_c) decreased. It can be noticed that the collapse settlement (S_c) significantly increases with increasing the intensity of induced water (Q_w). Furthermore, it was discovered that the ratio of settlement of four footings ($N = 4$) to isolated footing ($N = 1$) remains constant when the intensity of induced water ($Q_w = 2$ to $3 \text{ cm}^3/\text{cm}^2$) increases, with a value of 0.63.

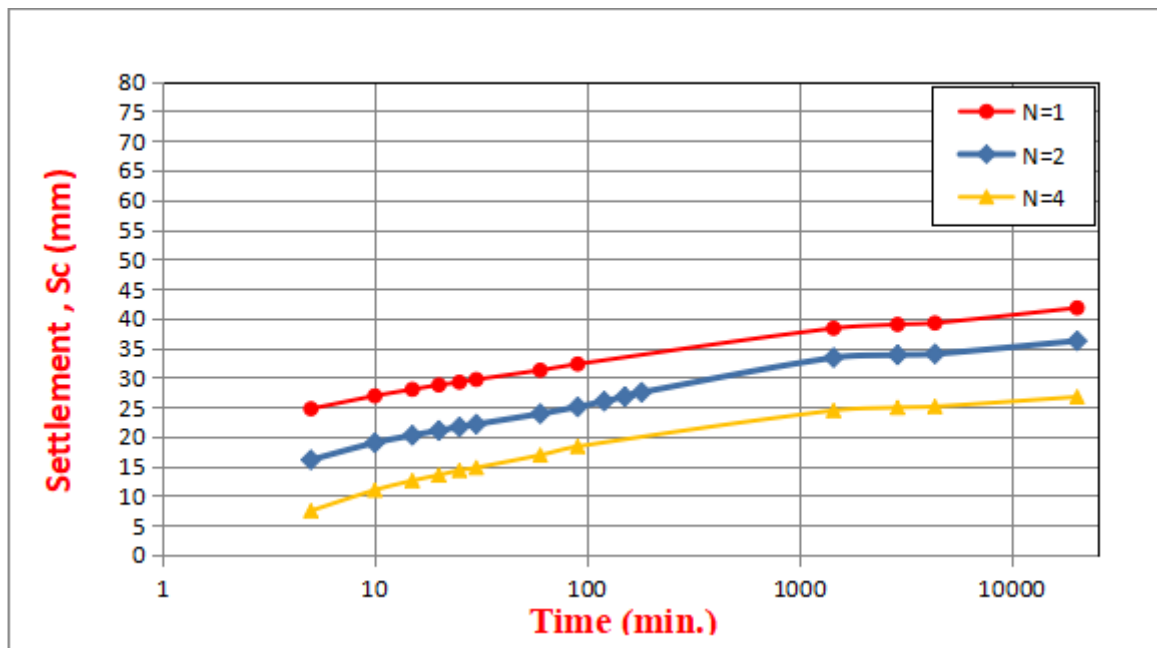


Figure (14): The settlement (S_c) with time for different number of footings (N) at $[\gamma_d=14.41 \text{ kN}/\text{m}^3$, $Q_w=2 \text{ cm}^3/\text{cm}^2$, $q=100 \text{ KN}/\text{m}^2$, $F=76.62\%$, $W_o=3.6\%$ and $B=7.6 \text{ cm}$].

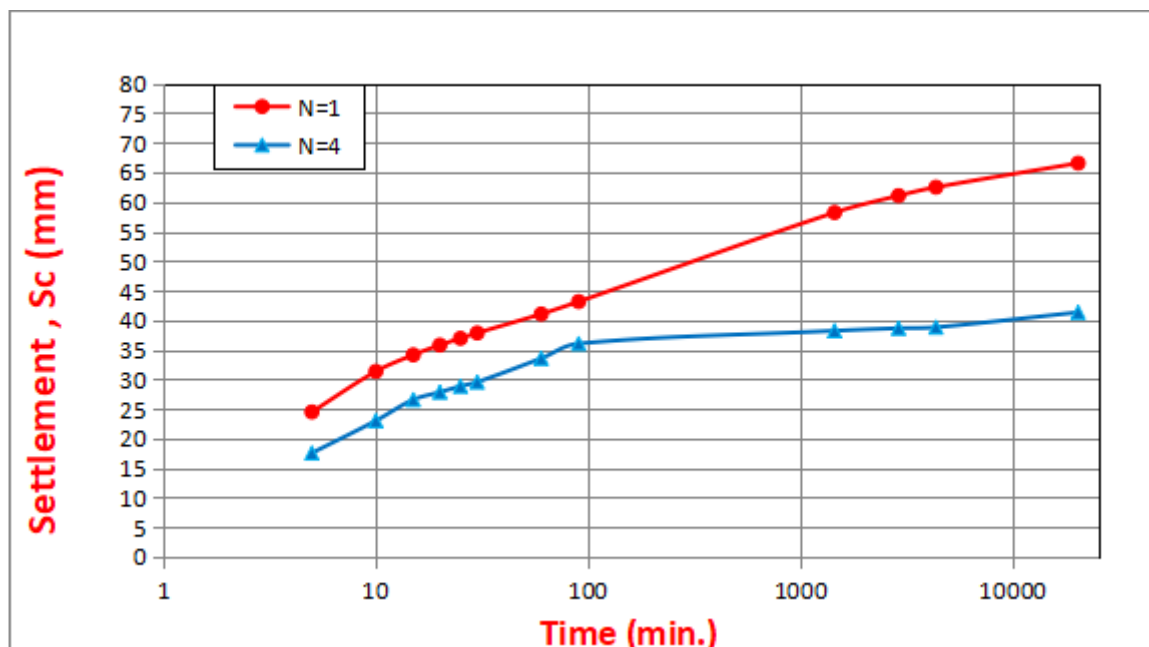


Figure (15): The settlement (S_c) with time for different number of footings (N) at $[\gamma_d=14.41 \text{ kN/m}^3$, $Q_w=3 \text{ cm}^3/\text{cm}^2$, $q=100 \text{ KN/m}^2$, $F=76.62\%$, $W_o=3.6\%$ and $B=7.6 \text{ cm}$].

4.2.1 Empirical Equation for Collapse settlement

Figure (16) shows the 3D regression analysis of the laboratory data using the Curve Expert Professional Program to generate equation (4), which can expect the value of collapse settlement for various parameters. The data revealed that the average ratio of expected to real collapse settlement is (1.00).

$$\delta = a * X_1^2 + b * X_2^2 + c * X_1 + d * X_2 + e \quad (4)$$

Where:

X_1 =Depth of wetting, D_w (cm)

$$X_2 = \frac{Q_w * W_o * q}{\gamma_d * \text{Fines} * N * \frac{B}{B_o}}$$

a	b	c	d	e
-0.00774	-1660	2.94	193	6.48

δ = the settlement (mm)

Q_w = the intensity of induced water (cm^3/cm^2)

Fines= the percentage of fines that passing sieve No. 200 (%)

W_o = the initial water content (%)

q = the applied stress (Kg/cm²).
 γ_d = the initial dry unit weight of the soil (Kg/cm³)
 B = the footing width (cm)
 B_o = the initial footing width (cm)
 N = number of footings.

The collapse settlement, S_c (mm)

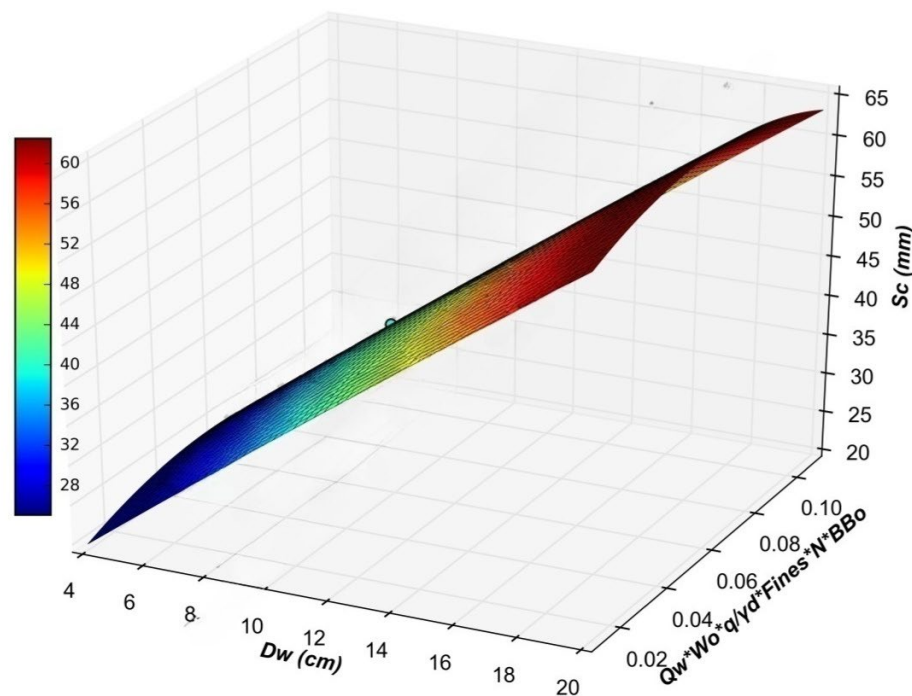


Figure (16): The Resulting 3D Graph of settlement vs $\frac{Q_w * W_o * q}{\gamma_d * \text{fines} * N * B / B_o}$ and D_w

5. NUMERICAL STUDY

Due to the difficulties in creating constitutive relations to characterize the behavior of collapsible soil, only a few numerical research on stress equilibrium and water flow in unsaturated soil have been identified. As a result, this study proposed a reliable procedure for simulating collapsible soil before, during, and after rainfall water. In this section, the finite element method PLAXIS 3D V21 was used to create a full model that simulates the same laboratory model capable of predicting the deformation of collapsible soil, and the results were compared to laboratory test results to check the ability of the proposed approach that was used in the numerical model for predicting settlement of collapsible soil. The model consists of collapsible soil beneath shallow footings as a result of rainwater infiltration. The soil bin utilized in the experiment has inside dimensions of 1000×1000 mm and a height of 1200 mm. In PLAXIS

3D software, the soil was represented as a typical elastic-perfect plastic model based on the Mohr-Coulomb failure criterion, while the foundations were designed as a square steel plates measuring (B = 76 mm) and 10 mm thick and the spacing between footings (S = 1.25 B). The footings were loaded with distributed uniform stress equal to 100 KN/m². Table (2) showed characteristics of collapsing soil and footings.

Table (2): the model parameters used for modeling the collapsible soil and footing.

<i>Parameter</i>	<i>Soil</i>	<i>Footing</i>
<i>Unit weight</i> (γ), KN/m ³	14.41	78.50
<i>Young's modulus (E),</i> KN/m ²	6032	2E6
<i>Poisson ratio (v)</i>	0.35	0.28
<i>Cohesion</i> (C) , KN/m ²	26.2	-----
<i>Angle of internal friction</i> (ϕ), °	43	-----
<i>Angle of dilatancy (ψ), °</i>	Φ-30	-----

The recommended procedure for modeling a collapsible soil and predicting collapse settlement in PLAXIS 3D V21 consists of the following steps:

(Initial phase): Characterized by a general phreatic level and zero steady-state pore pressure. The initial soil-effective stresses can be created using the K0 technique.

Phase (I): The footings were installed by changing the material characteristics of the footing cluster to fit the features that were introduced.

Phase (II): The external load on the footings was applied vertically as a surface load.

Phase (III): To take into consideration the volume change caused by wetness, the wetted depth of soil measured in the lab below the center of footings was divided into sublayers. The volumetric strain (ϵ_v) was computed for each layer using empirical equation (5) proposed by (Marei, 2019), which investigates the strain response when collapsible soil wetting at certain applied stress at wetting (P_w) and degree of saturation based on experimental tests.

Phase (III): Considering the differences in the stress state of each layer as known strength reductions in collapsible soil owing to rainfall water, the soil features of each layer were reassigned based on the distribution of water content of each layer obtained from laboratory experiments. The features of collapsible soil after wetting can be determined using direct shear box testing, as demonstrated in figures (17 and 18) (under publication).

$$\epsilon_{wp} = 11.8 * \exp^{-0.42 * \left(\frac{\ln(P_w)}{2.2} - 1.1 \right)^2 + (4.56 - \ln(S_w))^2} \quad (5)$$

Where:

ε_{wp} = the strain due to wetting (collapse) in %.

P_w = the applied stresses at wetting in kg/cm^2 .

S_w = the degree of saturation after wetting in %.

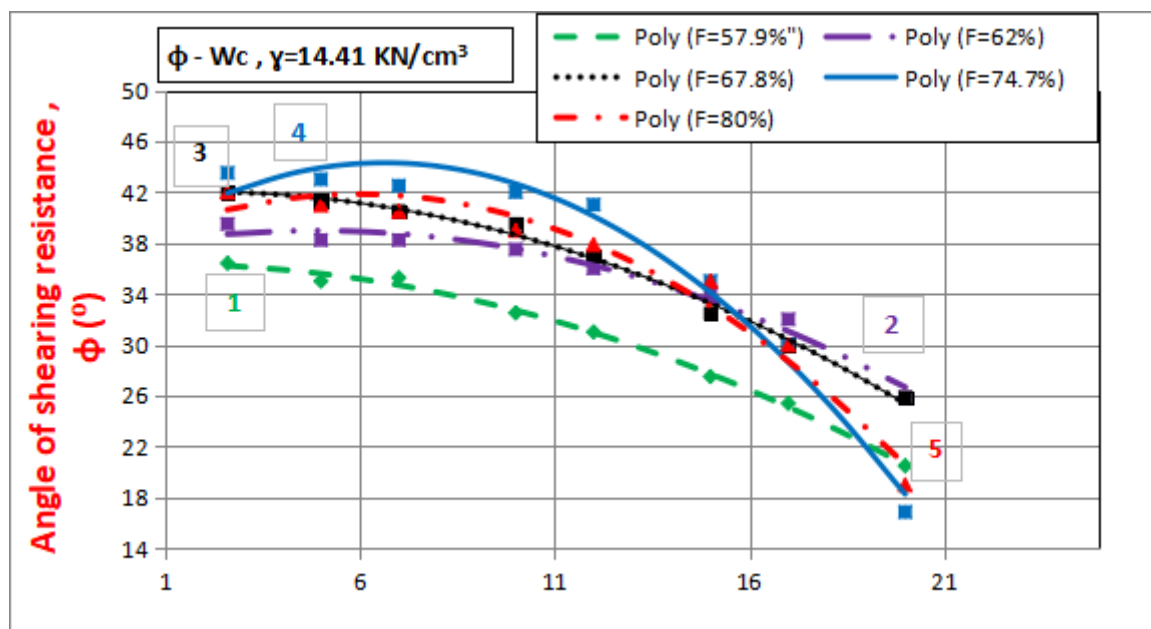


Figure (17): the relation between angle of friction and water content for different percentage of fines, at dry unit weight=14.41 KN/m^3

1	F=57.9%	$y = -0.0423X^2 + 0.0577X + 36.356$	$R^2=0.99$ 6
2	F=62%	$y = -0.0536X^2 + 0.521X + 37.7$	$R^2=0.97$ 65
3	F=67.8%	$y = -0.0496X^2 + 0.1654X + 41.928$	$R^2=0.99$ 25
4	F=74.7%	$y = -0.1457X^2 + 1.9339X + 37.881$	$R^2=0.97$ 97
5	F=80%	$y = -0.1078X^2 + 1.2855X + 38.001$	$R^2=0.96$ 84

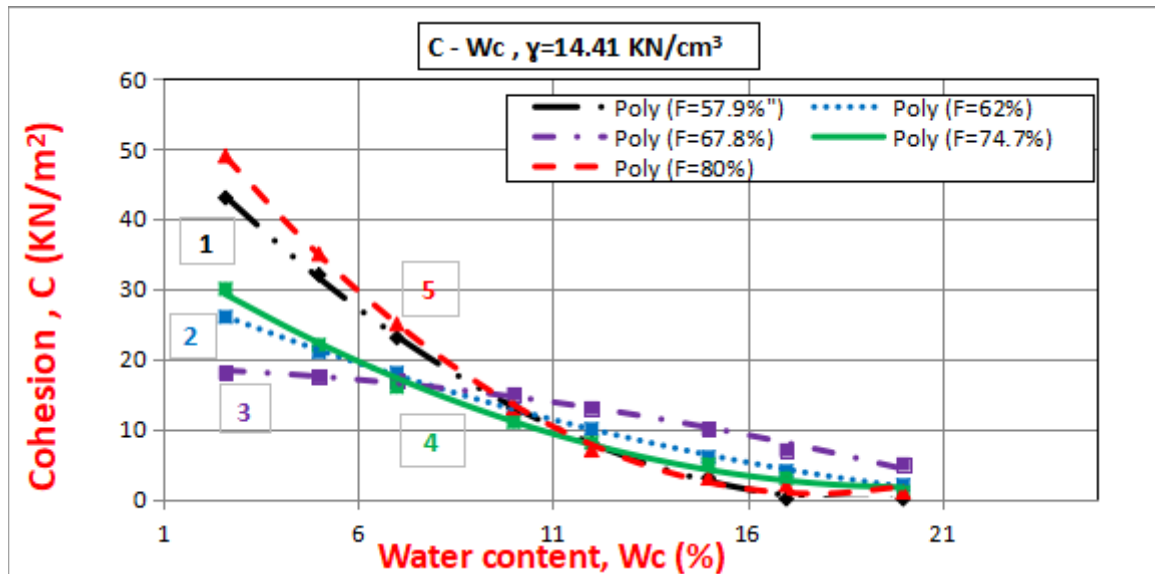
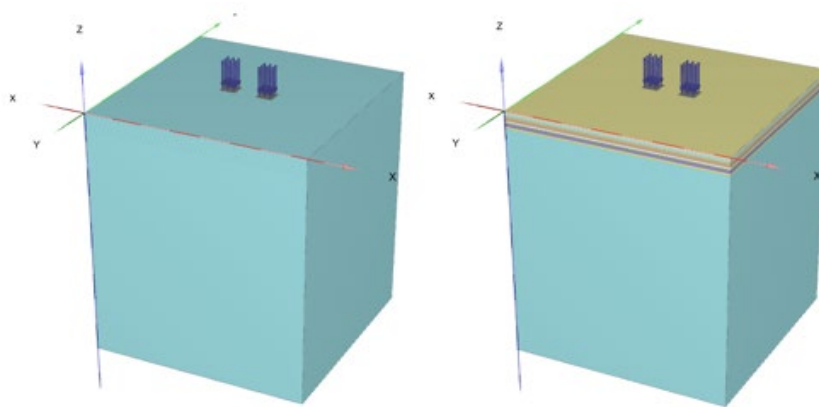


Figure (18): Relation between cohesion and water content for different percentages of fines, at dry unit weight=14.41 KN/m³

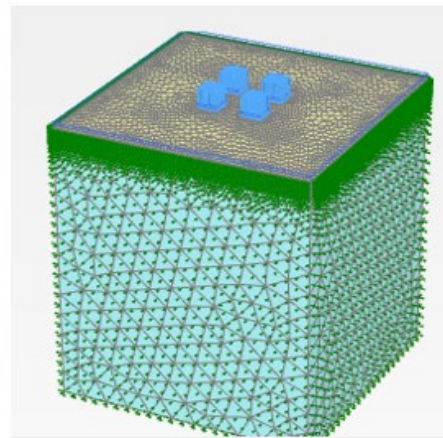
1	F=57.9%	$y = 0.157 X^2 - 6.0398 X + 57.826$	$R^2=0.99$ 95
2	F=62%	$y = 0.0394 X^2 - 2.2853 X + 31.715$	$R^2=0.99$ 91
3	F=67.8%	$y = -0.03 X^2 - 0.1301 X + 18.896$	$R^2=0.98$ 8
4	F=74.7%	$y = 0.0871 X^2 - 3.5529 X + 37.859$	$R^2=0.99$ 49
5	F=80%	$y = 0.2083 X^2 - 7.4134 X + 66.727$	$R^2=0.99$ 85

6. RESULT

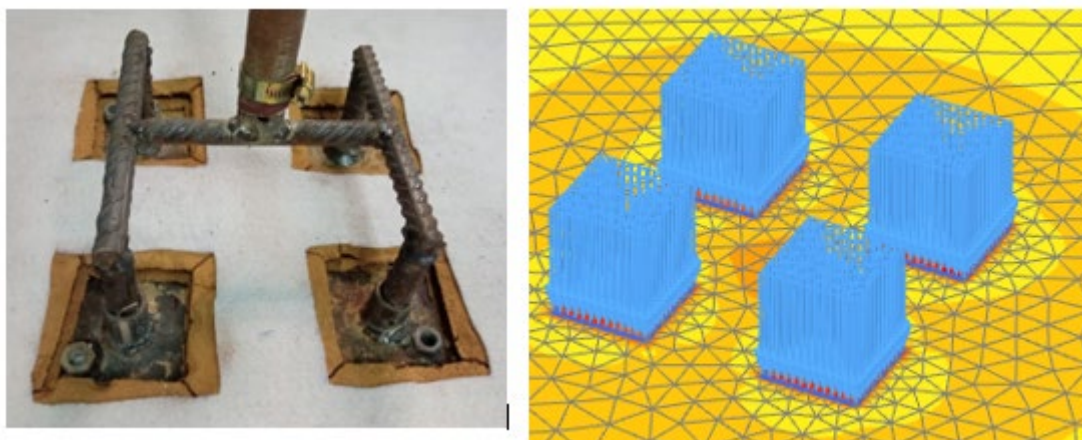
Figures (19 a) and (19 b) show a simulation of collapsible soil layers before and after being exposed to rainfall water, respectively. Figure (20) Compares the modeling of collapsible soil in the lab and PLAXIS. Figure (21) shows the deformation of collapsible soil following infiltration with rainfall water in the lab and PLAXIS ($Q_w = 3 \text{ cm}^3/\text{cm}^2$, $q = 100 \text{ KN/m}^2$, $B = 7.6 \text{ cm}$, $S = 1.25B$, $W_o = 3.6\%$, $F = 76.62\%$, and $\gamma_d = 14.41 \text{ KN/m}^3$). The results showed that the laboratory and numerical results were in good agreement. Figures (22) to (24) show soil deformation for various numbers of footings (N). It can be noticed that the deformation decreases as the number of footings increases. This is due to the water being distracted by the rising number of footings, and, as a result, the depth of wetting decreased, which is linked to the collapse settlement.



(a) Soil clusters before subjected to rainfall water (b) Soil clusters after subjected to rainfall water
Figure (19): the soil clusters before and after subjected to rainfall water for number of footings (N=2).



(a) Soil clusters subjected to rainfall water in lab (b) Soil clusters subjected to rainfall water in PLAXIS
Figure(20): the modeling of collapsible soil in the lab and PLAXIS.



(a) Soil clusters after subjected to rainfall water in lab (b) Soil clusters after subjected to rainfall water in PLAXIS

Figure (21): the deformation of soil clusters after subjected to rainfall water in lab and PLAXIS.

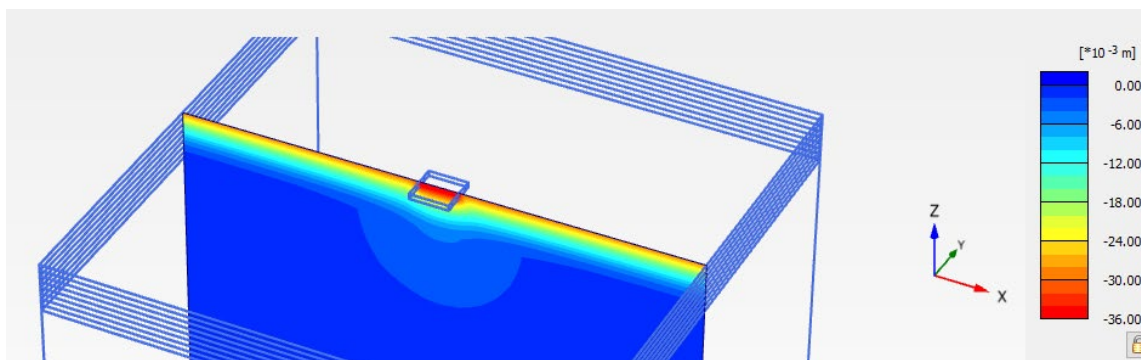


Figure (22): the deformation of soil clusters beneath the footing center at [N=1, $Q_w=2 \text{ cm}^3/\text{cm}^2$, $q=100 \text{ KN/m}^2$, $\gamma_d=14.41 \text{ KN/m}^3$, $W_o=3.6\%$, $F=76.62\%$ and $B=7.6 \text{ cm}$].

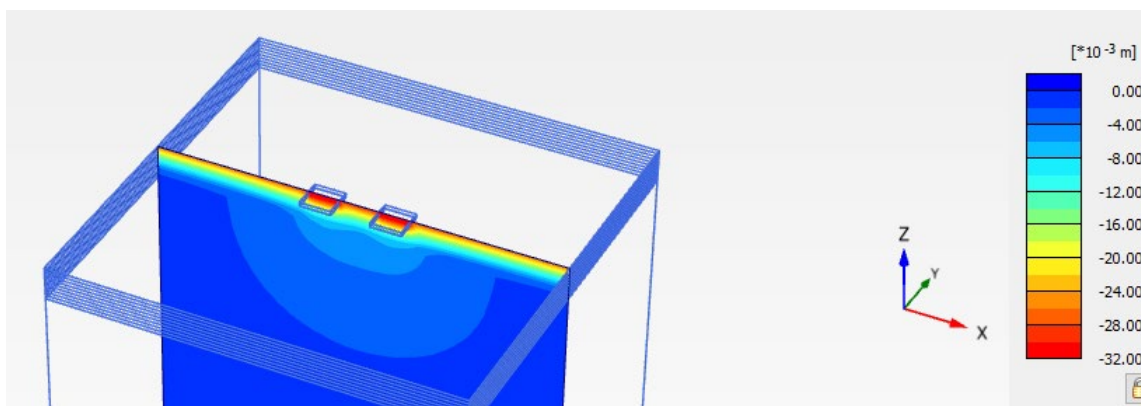


Figure (23): the deformation of soil clusters beneath the footing center at [N=2, $Q_w=2 \text{ cm}^3/\text{cm}^2$, $q=100 \text{ KN/m}^2$, $\gamma_d=14.41 \text{ KN/m}^3$, $W_o=3.6\%$, $F=76.62\%$ and $B=7.6 \text{ cm}$].

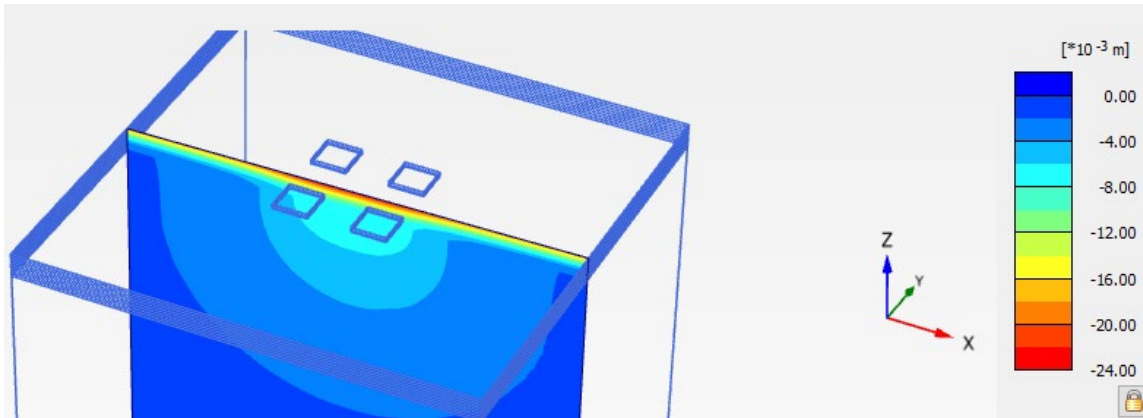


Figure (24): the deformation of soil clusters beneath the footing center at $[N=4, Q_w=2 \text{ cm}^3/\text{cm}^2, q=100 \text{ KN/m}^2, \gamma_d=14.41 \text{ KN/m}^3, W_o=3.6\%, F=76.62\% \text{ and } B=7.6 \text{ cm}]$.

7. COMPARISON BETWEEN EXPERIMENTAL AND NUMERICAL RESULTS

Figures (25 and 26) compare settlement values obtained from laboratory testing, empirical equation (4), and PLAXIS 3D V21 simulation model for all parametric investigations, dependent on actual measurements for the distribution of water content and depth of wetting during the tests. The results revealed a good agreement among the laboratory, empirical equation (4), and PLAXIS 3D V21 model for estimations of collapse settlement.

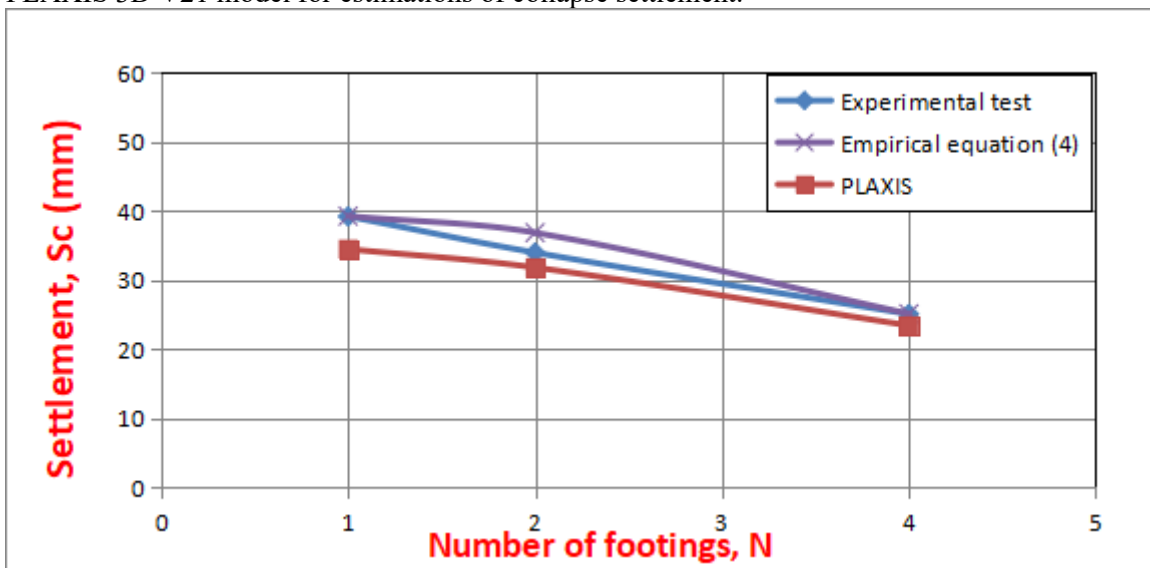


Figure (25): the settlement obtained from laboratory tests, empirical equation (4), and PLAXIS 3D V21 model for different number of footings (N) at $[\gamma_d=14.41 \text{ kN/m}^3, Q_w=2 \text{ cm}^3/\text{cm}^2, q=100 \text{ KN/m}^2, F=76.62\%, W_o=3.6\% \text{ and } B=7.6 \text{ cm}]$.

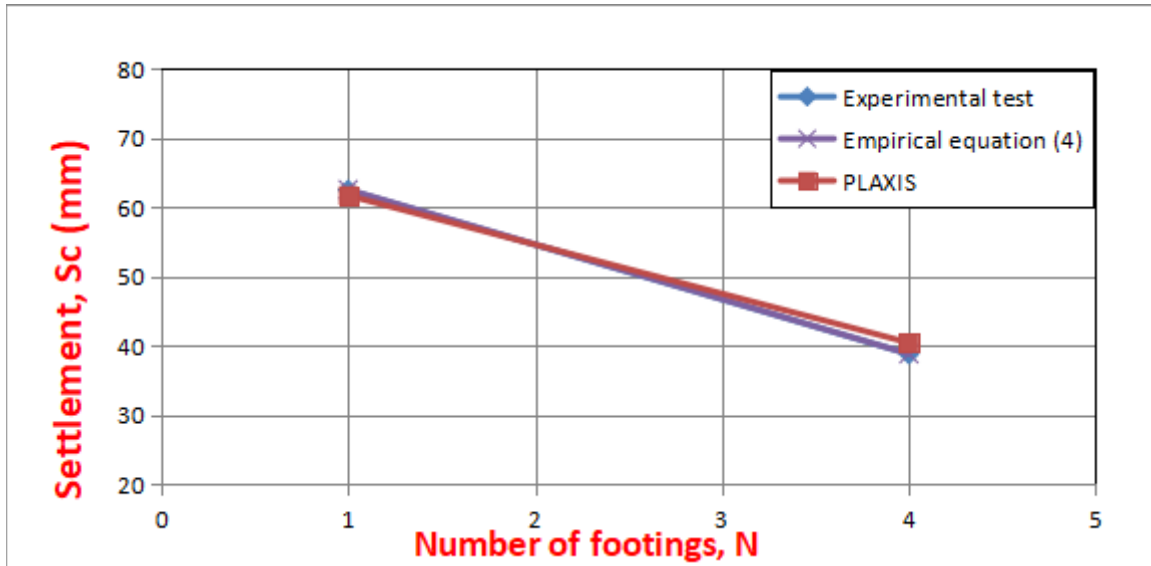


Figure (26): the settlement obtained from laboratory tests, empirical equation (4), and PLAXIS 3D V21 model for different number of footings (N) at [$\gamma_d=14.41$ kN/m³, $Q_w=3$ cm³/cm², $q=100$ KN/m², $F=76.62\%$, $W_o=3.6\%$ and $B=7.6$ cm].

8. LIMITATIONS

Based on this study which carried out on two groups of footings (one of 2 footings and the other of 4 footings), the proposed empirical equations performed well under the following conditions:

$\gamma_d = 14.41$ KN/m³, $W_o=3.6\%$, $Q_w=2$ to 3 cm³/cm², $Fines=76.62\%$, $q=100$ KN/m², $N= 1, 2$ and 4 , $S=1.25$ B and $B=7.6$ cm.

9. CONCLUSION

This study investigate the behavior of the loaded square group of footings models rested on the collapsible soil and the challenge of determining and locating a suitable tool to compute collapse settlement, especially induced by wetting the soil with rainfall water. Several results are described below:

[1] Based on experimental data, an empirical equation was developed to predict the change in water content within the wetted depth with the different parameters:

$$W_c = [a + b * X_1 + c * X_2 + d * X_1^2 + e * X_2^2 + f * X_1^3 + g * X_2^3 + h * X_1 * X_2 + i * X_1^2 * X_2 + j * X_1 * X_2^2]$$

[2] The suggested empirical equation for calculating the depth of wetting is:

$$D_w = \frac{a + b * X}{1 + c * X + d * X^2}$$

[3] The proposed empirical equation for calculating the wetted density is:

$$K_w = \left[\frac{a + bX_1 + cX_2}{1 + dX_1 + eX_2} \right]$$

[4] The recommended empirical equation for estimating the collapse settlement with several parametric studies is:

$$\delta = a * X_1^2 + b * X_2^2 + c * X_1 + d * X_2 + e$$

[5] The depth of wetting (D_w) is directly proportional to the intensity of induced water (Q_w) and inversely proportional to the number of footings (N).

[6] The water content distribution (W_c) was increased with increasing of the intensity of induced water (Q_w) and decreased with number of footings (N).

[7] The collapse settlement (S_c) is directly proportional to the intensity of induced water (Q_w) and inversely proportional to the number of footings (N).

[8] The decreasing in collapse settlement (S_c) with increasing number of footings (N) can explain why the measurements that reported by (Houston et al., 2002), (Ali, 2021) and (Fattah and Dawood, 2020) were found in the field are smaller than those measured in the laboratory, as a result of the effect of group of footings in the field.

[9] The behavior of a group of footings should take into account geotechnical engineers, which may be minimized in cost by changing the suggested collapsibility treatment method and the foundation type.

[10] The recommended procedure enables geotechnical engineers to simulate the collapsible soil before, during and after rainfall water using the finite element technique.

[11] The numerical model was compared with the results of laboratory tests of collapsible soil beneath shallow footings with rainwater infiltration to check the reliability of the presented model, and it was found a good agreement between the experimental results, numerical model and empirical equation (4).

10. LIST OF SYMBOLS

W_c: the distribution of water content (%).

W_o: the initial water content (%).

D_w : the depth of wetting (cm).

S_c: the collapse settlement (mm)

Q_w : the intensity of induced water (cm³/cm²).

F: the percentage of fines that passing sieve No. 200 (%).

W_o: the initial water content (%).

q : the applied stress (Kg/cm²).

γ_d: the initial dry unit weight of the soil (Kg/cm³)

γ_w: the wetted density (Kg/cm³)

B : the footing width (cm)

B_o: the initial footing width (cm)

N: the number of footings.

S: the spacing between footings (cm).

C: the cohesion (KN/m²).

Φ: the angle of friction (°).

ϵ_{wp} : the strain due to wetting collapse (%).
 P_w : the applied stresses at wetting (kg/cm²).
 S_w :the degree of saturation after wetting (%).

E : the modulus of elasticity (KN/m²).
 ν : the Poisson ratio
 ψ : the angle of dilatancy (°).

11. REFERENCES

- [1] Abdrabbo, F.M. and Abdelaziz, T.M. (2006): “**Study of the Infiltration of Water Through Collapsible Soil**”, The Fourth International Conference on Unsaturated Soils, Arizona. [https://doi.org/10.1061/40802\(189\)85](https://doi.org/10.1061/40802(189)85)
- [2] Behzad Kalantari, (2013): “**Foundations on collapsible soils: A review**”, Proceedings of the Institution of Civil Engineers - Forensic Engineering 166(2):57-63. [DOI:10.1680/feng.12.00016](https://doi.org/10.1680/feng.12.00016)
- [3] Choudhury, C., Bharat, T.V. (2015): “**Collapse behavior of clay soil under one-dimensional (1D) compression condition**”, In: 50th Indian Geotechnical Conference, Maharashtra, India
- [4] El-Ehwany, M. and Houston, S.L. (1990): “**Settlement and moisture movement in collapsible soils**”, Journal of Geotechnical Engineering, vol.116, No.10 pp.1521-1535.
- [5] Houston, S.L., Houston, W.N., Zapata, C.E., Lawrence, C. (2001): “**Geotechnical engineering practice for collapsible soils**”, Geotech. Geol. Eng. 19(3), 333–355. <https://doi.org/10.1023/A:1013178226615>
- [6] Houston, S.L., Houston W.N., Lawrence, C.A. (2002): “**Collapsible soil engineering in highway infrastructure development**”, J. Transp. Eng. 128(3), 295–300. [https://doi.org/10.1061/\(asce\)0733-947x\(2002\)128:3\(295\)](https://doi.org/10.1061/(asce)0733-947x(2002)128:3(295))
- [7] Lawton, E.C., Frigaszy, R.J., Hetherington, M.D.(1992): “**Review of wetting-induced collapse in compacted soil**”, J. Geotech. Eng. 118(9), 1376–1394. [https://doi.org/10.1061/\(asce\)0733-9410\(1992\)118:9\(1376\)](https://doi.org/10.1061/(asce)0733-9410(1992)118:9(1376))
- [8] Mohamed Marei (2019): “**The Effect of Applied Stress and Degree of Saturation of Soil on Collapse Settlement**”, a thesis submitted to Arab Academy for Science, Technology and Maritime Transport in partial fulfillment of the requirements for Master Degree.
- [9] Mohammed Y. Fattah and Basma A. Dawood (2020): “**Time-dependent collapse potential of unsaturated collapsible gypseous soils**”, World Journal of Engineering 17/2, 283–294.
- [10] Murthy, V.N.S. (2010): “**Soil mechanics and foundation engineering**”, New Delhi, CBS publishers and distributors.
- [11] Naema A. Ali (2021): “**Egyptian Collapsible Soils, Case Study- Region Affected by Varying Moisture Content**”, International Journal of Engineering Research & Technology (IJERT), ISSN: 2278-0181, Vol. 10 Issue 05. <http://www.ijert.org/>



[12] Naema A. Ali (2021): **“Practical Engineering Behavior of Egyptian Collapsible Soils, Laboratory and In Situ Experimental Study”**, Open Journal of Civil Engineering, 290-300, ISSN Online: 2164-3172. <https://doi.org/10.4236/ojce.2021.113017>

[13] Walsh, K.D; Houston, W.N. and Houston, S.L. (1993): **“Evaluation of in-place wetting using soil suction measurements”**, Journal of Geotechnical Engineering, vol.119, No.5, pp. 862-873.
[https://doi.org/10.1061/\(asce\)0733-9410\(1993\)119:5\(862](https://doi.org/10.1061/(asce)0733-9410(1993)119:5(862)



Arab Academy for Science, Technology, and Maritime Transport
The International Maritime and Logistics Conference “MARLOG 14”
“Artificial Intelligence Implementations
Towards Shaping the Future of Digital World”
23 – 25 February 2025

